iJRASET
International Journal For Research in Applied Science and Engineering Technology

INTERNATIONAL JOURNAL FOR RESEARCH

IN APPLIED SCIENCE & ENGINEERING TECHNOLOGY

Volume: 13 **Issue:** III **Month of publication:** March 2025

DOI: https://doi.org/10.22214/ijraset.2025.67227

www.ijraset.com

Call: 08813907089 | E-mail ID: ijraset@gmail.com

International Journal for Research in Applied Science & Engineering Technology (IJRASET)
ISSN: 2321-9653; IC Value: 45.98; SJ Impact Factor: 7.538
Volume 13 Issue III Mar 2025- Available at www.ijraset.com

Theoretical Examination of the Trembling Motion of Dirac Electrons on the Surfaces of Single and Multilayer Armchair Graphene Nanoribbons

Bashar Hawi Azeez Abu-Gebaz
Department of Physics, College of Science, AL-Muthanna University, AL-Muthanna, IRAQ

Abstract: ***The phenomenon of trembling motion, known as Zitterbewegung (ZBW) in German, has intrigued scientists for many years. This research report offers a theoretical analysis of this occurrence in armchair-type graphene strips using the long-wave model, determining the position operator for the $\hat{x}$ and $\hat{y}$ directions according to the Heisenberg representation. The Gaussian distribution function was used as a representation of the pseudo-spin wave function. The influence of the graphene nanoribbon's width and the wave vector kx on the oscillation values of this phenomena, together with the multiplicity of graphene layers, was examined. This particular graphene nanoribbon was selected because to its minimal edge effects, allowing it to function as a semiconductor material with a controllable energy gap. Consequently, this phenomenon may be realised via the interference between the conduction and valence energy bands. A series of analytical and numerical mathematical computations were performed, resulting in the following findings: This phenomenon was first seen in this sort of graphene nanoribbons, occurring within around 30 femtoseconds for both orientations and varying values of α and β. The hexagonal graphene lattice has a likelihood of harbouring electrons. Secondly, the findings indicated that the oscillation of the electron wave packet is transitory and bidirectional, exhibiting semi-regular periodicity for widths of $M = 5$ and $M = 10$ across all layers. The oscillation value rises as the breadth of the wave packet diminishes. Thirdly, when the number of graphene layers rises, an area referred known as the Astrach region emerges owing to electron transport between the layers. The influence of the hopping energy parameter is evident here. This study work offers theoretical insights into the Zitterbewegung phenomena in graphene strips, representing a modest addition to the field.***

Keywords: Graphene; Armchair Graphene Nanoribbon (AGNRs); Trembling motion; Wave packet of electrons; ZBW.

I. INTRODUCTION

It was in 1930 that Schrodinger made the prediction that free electrons in a vacuum will experience a phenomenon known as Zitterbewegung (ZBW) [1]. Since the Dirac equation's electron velocity operator does not commute with the Hamiltonian, we may say that the electron velocity is not a motion equation constant. The solutions to the Dirac equation for a relativistic electron in free space are what give rise to the term "thumping velocity," which is used to describe the velocity of an electron when there is no effective external field present [1,2]. In relativistic quantum systems, the wave packet is a distinguishing feature that differentiates it from nonrelativistic quantum systems. The wave packet's location oscillates over time owing to the strong coupling between the pseudo-spin degree of freedom and momentum [3]. This oscillation is a typical feature of relativistic quantum systems. despite the fact that this phenomenon has received a considerable amount of theoretical attention from the point of view of relativistic theory. The time development of the expected values of certain physical observables, such as location, velocity, current, and spin angular momentum, is a manifestation of the oscillatory dynamic that pertains to the centre of a free wave packet. Zitterbewegung motion's signature frequency is defined by the energy difference between the positive and negative states. This frequency is of the order of $2m_0c^2/\hbar$, where m_0 is the mass of the electron, c is the velocity of light, and $\hbar$ is the Planck constant. But oscillation amplitudes are on the order of the Compton wavelength. So, this is equivalent to very high oscillation frequencies with very tiny amplitudes, both of which are inaccessible using the methods of experimentation that are now in use [4]. Graphene, which is a single layer of a honeycomb lattice of carbon atoms with unique electronic characteristics, has been the subject of a recent reexamination of the Zitterbewegung phenomenon. This is because low-energy electrons in graphene function as quasi-relativistic particles [5]. Graphene exemplifies a unique system characterised by linear dispersion at low energy, facilitating a bridge between the high-energy domain and the low-energy condensed matter realm. In spite of the fact that graphene has intriguing characteristics, its applications in semiconductor circuits are restricted due to the fact that the energy gap is very narrow.

©IJRASET: All Rights are Reserved

However, when a two-dimensional sheet of graphene is sliced into a semi-one-dimensional sheet, graphene may be produced. The production of so-called graphene nanoribbons will result from this process. These nanoribbons may be divided into two primary categories: armchair and zigzag. The geometry of the edge along the nanoribbon is what determines this categorisation. By using the weak van der Waals forces, it is feasible to organise the various layers of graphene in a manner that allows them to interact with one another. While the Bernal structure (ABABA...) is the most common ordering of graphite layers, other arrangements are conceivable, and are indicated by the composition (ABCABC A...). Because of this arrangement, graphite formations are said to have a defect or distortion in their crystal structure. Graphite has an interlayer distance of about $h = 0.335\,nm$, which is much larger than the distance between carbon atoms in a single layer $a = 0.124\,nm$.The difference is that this distance is really large.Due to the fact that the velocity operator does not commute with the Hamiltonian in the systems, the Zitterbewegung phenomenon was thought to be responsible for the minimal conductivity that was seen in the graphene system in the early research. Using the connection between the theory of the energy bands in narrow-gap semiconductors (NGS) and the free Dirac relativistic equation for electrons [6]. Zawadzki et al. conducted research on ZB in NGS in the year 2005. For a free electron, they discovered that the amplitude and frequency of the oscillation were much more favourable than those in a vacuum [7-8]. At the same time, Schliemann and colleagues have conducted an in-depth investigation of the ZBW of an electron in III-V zinc-blende semiconductor QWs when the SOI was present. The aforementioned discoveries served as the impetus for further theoretical study on the ZBW of electrons in a variety of condensed matter systems [9,10]. Graphene, graphene nanoribbons, and carbon nanotubes are examples of carbon nanomaterials that possess remarkable physical and chemical characteristics [11,12]. These qualities have the potential to be used in the development of promising electronic nanotechnologies [13,14]. It was for the first time that it was emphasised theoretically that the minimum conductivity of graphene may be described in terms of the phenomena ZBW [15]. Consequently, a large number of academics are interested in it. In 2008, researchers looked at how charge carriers changed time evolution and measured their ZBW in semiconducting carbon nanotubes with cylindrical symmetry, monolayer graphene, and bilayer graphene [16]. Ghosh et al. conducted a theoretical investigation of the occurrence of ZBW as well as the advancement of the wave packet over time in zigzag graphene nanoribbon (ZGNR) [3]. They highlighted the fact that the connection between the bulk states and edge states has fascinating characteristics, and they also made the observation that the oscillation in position happens along the direction of the wave packet propagation, which is not possible in the infinite graphene sheets and semiconductor nanowires. Majid and Savinskii [17,18], along with Majid and Alla [19-21], examined the impact of different pseudospin polarisations on wave-packet dynamics in monolayer graphene, carbon nanotubes, and graphene nanoribbons, focussing on the initial wave function and the ZBW phenomenon. They did this by using the Heisenberg representation [22]. Also, they investigated the phenomenon of ZBW. The long wave approximation and the Heisenberg representation are used in order to conduct a theoretical investigation of the time evolution of the wave packet in bilayer graphene. Reference [23] looks at how a low-energy two-dimensional Gaussian wave packet in ABC-stacked n-layer graphene (ABC-NLG) changes over time. This wave packet is a Gaussian function with two dimensions. Time evolution of the projected value of the position operator (ZBW) in the multilayer armchair graphene nanoribbon (MLAGNR) is considered analytically and numerically in the present work. The mathematical representation is located in the second section. In the third section, we provide our results for all conceivable parameters that influence the time evolution of the MLAGNRs.

II. A THEORETICAL FRAMEWORK

For the long wave model, the following is the effective low energy Hamiltonian of graphene, which is located at the K point in the first Brillouin zone.[17]:

$$\widehat{H} = V_F(\sigma_x \hat{p}_x + \sigma_y \hat{p}_y) \quad (1)$$

Following is a description of the generalised version of graphene that is present in multilayers when there are no external fields present:

$$\widehat{H}^n = \frac{{V_F}^n}{\gamma^{n-1}}\left(\sigma_x {\hat{p}_x}^n + \sigma_y {\hat{p}_y}^n\right) \quad (2)$$

As illustrated in Fig.1, the Fermi velocity is denoted by V_F, while the Pauli matrices and momentum effects are represented by σ_x and σ_y. The hopping energy between the graphene layers is denoted by γ^n, which is equal to $\gamma = 0.377$ meV [18]. The number of graphene layers is denoted by n. Fig.2 depicts the structural diagram of an armchair graphene nanoribbon, which has a length of L and a width of D. On the ribbon, the width is shown as a function of two carbon atoms per unit cell, and it is represented by dashed lines along the $y - axis$ of the ribbon.[21]:

$$D = \frac{M}{4}\sqrt{3}a_o \quad (3)$$

a_o represents the graphene lattice constant in this formula. Here we can see the energy spectrum of a layered armchair graphene nanoribbon with widths D:

$$E_{ks}^{n} = \frac{sV_F{}^n \hbar^n \mathcal{E}^n}{\gamma^{n-1}}, \mathcal{E} = \sqrt{1 + 4\cos(k_q)\cos\frac{k}{2} + 4\cos^2 k_q} \quad (4)$$

where $k_q = \frac{2}{\sqrt{3}a_o}\frac{q}{M+1}\pi, q = 1,2,3,\ldots M, S = \pm 1$

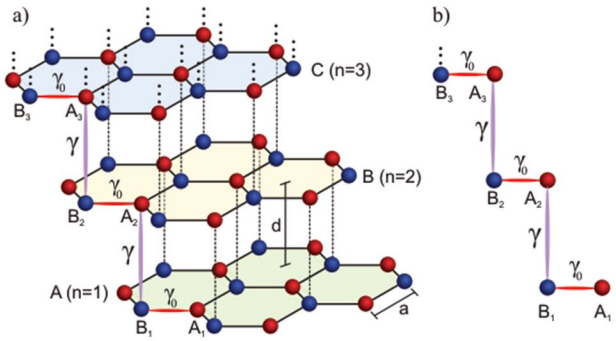

Fig.1. (a) Illustration of the ABC structure, which consists of three layers of graphene stacked rhombohedra. The red (A) and blue (B) circles represent the two asymmetric carbon sublattices present in each particular layer, respectively. (b) Schematic representation of the trilayer graphene stacked in an ABC pattern with interlayer hopping between the first nearest neighbors equal to zero and interlayer hopping energy between Ai and Bi+1 sites for each layer [23].

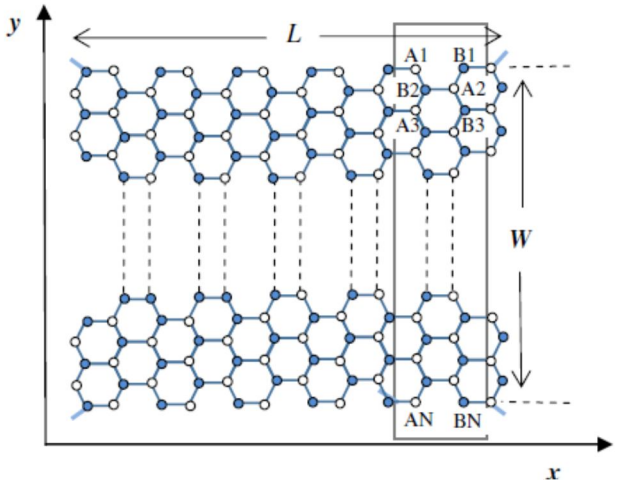

Fig 2. Armchair graphene nanoribbon of length d and width D [21].

It is possible to express the spinor wave function of the Hamiltonian with respect to eq.2 as follows:

$$\left|\psi_{kqsn}\right\rangle = \frac{1}{2\pi\sqrt{DL}} exp(ikx + ik_q y)\frac{1}{\sqrt{2}}\begin{pmatrix} A_{nk} \\ Sn \end{pmatrix}, A_{nk} = \frac{k - ik_q}{\sqrt{k^2 + k_q^2}} \quad (5)$$

where the integer n represents the number of individual quantum states that make up the band. Under the assumption that the graphene nanoribbon is the core of the original wave packet, we may say that it is a superposition of the spinor wave functions. The initial momentum is denoted by k_{x0}, while the initial momentum is denoted by k_{y0}:

$$\left|\psi(0)\right\rangle = Bexp\left(-\frac{x^2}{2d^2} - \frac{y^2}{2d^2} + ik_{x0}x + ik_{y0}y\right)\begin{pmatrix}\alpha \\ \beta\end{pmatrix} \quad (6)$$

In our current calculations, the parameters α and β indicate the polarisation of the pseudo-spin. These parameters provide the connection between the components of the pseudo-spin in the wave function.

Additionally, d represents the width of the localised wave packet on the surface of the ribbon. For the wave packet, it is not difficult to get an arbitrary starting quantum state by using the pseudospin's function, as shown in the following:

$$|\psi(0)\rangle = \sum_{n,s}\int_{-\infty}^{\infty} a_{kns}|\psi_{kns}\rangle, a_{kns} = \langle\psi_{kns}|\psi(0)\rangle \quad (7)$$

where a_{knS} the expansion coefficients of the quantum state are represented, which may be described in the following way:

$$a_{knS} = \frac{d}{\sqrt{\alpha^2+\beta^2}\sqrt{2\pi}\sqrt{DL}}(\alpha A_{nk}^* + \beta Sn)exp\left(-\left(\frac{\left(k-k_{x_\circ}\right)^2 d^2}{2}\right)\right)exp\left(-\left(\frac{\left(k_n-k_{y_\circ}\right)^2 d^2}{2}\right)\right) \quad (9)$$

It is well knowledge that the Heisenberg representation, which may be defined as follows, is responsible for determining the average value of any physical quantity P at time t.

$$\langle P(t)\rangle = \langle\psi(0)|\hat{P}(t)|\psi(0)\rangle \quad (10)$$

$$\langle P(t)\rangle = \sum_{s,\bar{s}}\int dk\, a_{kns}^*\, a_{knsN}\langle\psi_{kns}|\hat{P}(t)|\psi_{\bar{k}\bar{n}\bar{s}}\rangle \quad (11)$$

In both the longitudinal and transversal directions, the following Heisenberg operators identify the position of the AGNR for the multilayer layers:

$$\hat{x}^n(t) = x^n(0) + \frac{(V_F{}^n)^2\hat{p}_x^n n!}{\hat{H}\gamma^{n-1}}t + \frac{iV_F{}^n\hbar n!}{2\hat{H}\gamma^{n-1}}\left(\hat{\sigma}_x(0) - \frac{V_F{}^n\hat{p}_x^n}{\hat{H}\gamma^{n-1}}\right)\left(e^{-\frac{2iHt}{\hbar}} - 1\right) \quad (12)$$

$$\hat{y}^n(t) = y^n(0) + \frac{(V_F{}^n)^2\hat{p}_y^n n!}{\hat{H}\gamma^{n-1}}t + \frac{iV_F{}^n\hbar n!}{2\hat{H}\gamma^{n-1}}\left(\hat{\sigma}_y(0) - \frac{V_F{}^n\hat{p}_y^n}{\hat{H}\gamma^{n-1}}\right)\left(e^{-\frac{2iHt}{\hbar}} - 1\right) \quad (13)$$

$$a_{kns}^* a_{kns'} = \frac{d^2}{(|\alpha|^2+|\beta|^2)2\pi DL}(\alpha A_{nk} + \beta Sn)(\alpha A_{nk}^* + \beta S'n)e^{-(k-k_{x0})^2 d^2}e^{-\left(k_n-k_{y0}\right)^2 d^2} \quad (14)$$

In conclusion, we arrive at the following formula for calculating the average values of the longitudinal and transversal components of the location of the AGNR for n layers:

$$x(t) = \sum_{S,S'}\int dk\,\{\mu(\alpha A_{nk} + \beta Sn)(\alpha A_{nk}^* + \beta S'n)\}\left\{\left(\frac{A_{nk}^* A_{nk}+SS'n^2}{2}\right)\left(\frac{V_F^n k_x^n n!t}{S'\varepsilon^n}\right) + \frac{in!}{2S'\varepsilon^n}\left[\left(\frac{A_{nk}Sn+A_{nk}^* S'n}{2}\right) - \left(\frac{A_{nk}^* A_{nk}+SS'n^2}{2}\right)\left(\frac{k_x^n n!}{S'\varepsilon^n}\right)\right]\left[e^{\frac{-2iS'V_F^n\varepsilon^n}{\gamma^{n-1}}t} - 1\right]\right\} \quad (15)$$

$$y(t) = \sum_{S,S'}\int dk\,\{\mu(\alpha A_{nk} + \beta Sn)(\alpha A_{nk}^* + \beta S'n)\}\left\{\left(\frac{A_{nk}^* A_{nk}+SS'n^2}{2}\right)\left(\frac{V_F^n k_q^n n!t}{S'\varepsilon^n}\right) + \frac{in!}{2S'\varepsilon^n}\left[\left(\frac{i(A_{nk}Sn-A_{nk}^* S'n)}{2}\right) - \left(\frac{A_{nk}^* A_{nk}+SS'n^2}{2}\right)\left(\frac{k_x^n n!}{S'\varepsilon^n}\right)\right]\left[e^{\frac{-2iS'V_F^n\varepsilon^n}{\gamma^{n-1}}t} - 1\right]\right\} \quad (16)$$

where $\mu = \frac{d^2Z^2}{(|\alpha|^2+|\beta|^2)2\pi DL}e^{-(k-k_x)^2 d^2}e^{-(k_n-k_y)^2 d^2}, Z = \frac{1}{2\pi\sqrt{DL}}$

For each and every value of S and S', the following is the overall average value of the position operator's longitudinal and transversal components:

a) $S = +1\,, S' = +1$

$$x(t) = \int dk\,\{\mu(\alpha A_{nk} + \beta n)(\alpha A_{nk}^* + \beta n)\}\left\{\left(\frac{A_{nk}^* A_{nk}+n^2}{2}\right)\left(\frac{V_F^n k_x^n n!t}{\varepsilon^n}\right) + \frac{in!}{2\varepsilon^n}\left[\left(\frac{A_{nk}n+A_{nk}^* n}{2}\right) - \left(\frac{A_{nk}^* A_{nk}+n^2}{2}\right)\left(\frac{k_x^n n!}{\varepsilon^n}\right)\right]\left[e^{\frac{-2iV_F^n\varepsilon^n}{\gamma^{n-1}}t} - 1\right]\right\} \quad (17)$$

$$y(t) = \int dk\,\{\mu(\alpha A_{nk} + \beta n)(\alpha A_{nk}^* + \beta n)\}\left\{\left(\frac{A_{nk}^* A_{nk}+n^2}{2}\right)\left(\frac{V_F^n k_x^n n!t}{\varepsilon^n}\right) + \frac{in!}{2\varepsilon^n}\left[\left(\frac{i(A_{nk}N-A_{nk}^* n)}{2}\right) - \left(\frac{A_{nk}^* A_{nk}+n^2}{2}\right)\left(\frac{k_q^n n!}{\varepsilon^n}\right)\right]\left[e^{\frac{-2iV_F^n\varepsilon^n}{\gamma^{n-1}}t} - 1\right]\right\} \quad (18)$$

b) $S = -1\,, S' = -1$

$$x(t) = \int dk\,\{\mu(\alpha A_{nk} - \beta n)(\alpha A^*_{nk} - \beta n)\}\left\{\left(\frac{A^*_{nk}A_{nk}+n^2}{2}\right)\left(-\frac{V_F^n k_x^n n!t}{\varepsilon^n}\right) - \frac{in!}{2\varepsilon^n}\left[\left(\frac{-A_{nk}N - A^*_{nk}n}{2}\right) - \left(\frac{A^*_{nk}A_{nk}+n^2}{2}\right)\left(-\frac{k_x^n n!}{\varepsilon^n}\right)\right]\left[e^{\frac{2iV_F^n\varepsilon^n}{\gamma^{n-1}}t} - 1\right]\right\} \quad (19)$$

$$y(t) = \int dk\,\{\mu(\alpha A_{nk} - \beta n)(\alpha A^*_{nk} - \beta n)\}\left\{\left(\frac{A^*_{nk}A_{nk}+n^2}{2}\right)\left(\frac{-V_F^n k_x^n n!t}{\varepsilon^n}\right) - \frac{in!}{2\varepsilon^n}\left[\left(\frac{i(-A_{nk}N + A^*_{nk}n)}{2}\right) - \left(\frac{A^*_{nk}A_{nk}+n^2}{2}\right)\left(\frac{-k_q^n n!}{\varepsilon^N}\right)\right]\left[e^{\frac{2iV_F^n\varepsilon^n}{\gamma^{n-1}}t} - 1\right]\right\} \quad (20)$$

c) $S = +1\,, S' = -1$

$$x(t) = \int dk\,\{\mu(\alpha A_{nk} + \beta n)(\alpha A^*_{nk} - \beta n)\}\left\{\left(\frac{A^*_{nk}A_{nk}-n^2}{2}\right)\left(-\frac{V_F^n k_x^n n!t}{\varepsilon^n}\right) - \frac{in!}{2\varepsilon^n}\left[\left(\frac{A_{nk}n - A^*_{nk}n}{2}\right) - \left(\frac{A^*_{nk}A_{nk}-n^2}{2}\right)\left(-\frac{k_x^n n!}{\varepsilon^n}\right)\right]\left[e^{\frac{2iV_F^n\varepsilon^n}{\gamma^{n-1}}t} - 1\right]\right\} \quad (21)$$

$$y(t) = \int dk\,\{\mu(\alpha A_{nk} + \beta n)(\alpha A^*_{nk} - \beta n)\}\left\{\left(\frac{A^*_{nk}A_{nk}-n^2}{2}\right)\left(-\frac{V_F^n k_x^n n!t}{\varepsilon^n}\right) - \frac{in!}{2\varepsilon^n}\left[\left(\frac{i(A_{nk}n - A^*_{nk}n)}{2}\right) - \left(\frac{A^*_{nk}A_{nk}-n^2}{2}\right)\left(-\frac{k_q^n n!}{\varepsilon^n}\right)\right]\left[e^{\frac{2iV_F^n\varepsilon^n}{\gamma^{n-1}}t} - 1\right]\right\} \quad (22)$$

d) $S = -1\,, S' = +1$

$$x(t) = \int dk\,\{\mu(\alpha A_{nk} - \beta n)(\alpha A^*_{nk} + \beta n)\}\left\{\left(\frac{A^*_{nk}A_{nk}-n^2}{2}\right)\left(\frac{V_F^n k_x^n n!t}{\varepsilon^n}\right) + \frac{in!}{2\varepsilon^n}\left[\left(\frac{-A_{nk}n + A^*_{nk}n}{2}\right) - \left(\frac{A^*_{nk}A_{nk}-n^2}{2}\right)\left(\frac{k_x^n n!}{\varepsilon^n}\right)\right]\left[e^{\frac{-2iV_F^n\varepsilon^n}{\gamma^{n-1}}t} - 1\right]\right\} \quad (23)$$

$$y(t) = \int dk\,\{\mu(\alpha A_{nk} - \beta n)(\alpha A^*_{nk} + \beta n)\}\left\{\left(\frac{A^*_{nk}A_{nk}-n^2}{2}\right)\left(\frac{V_F^n k_x^n n!t}{\varepsilon^n}\right) + \frac{iN!}{2\varepsilon^N}\left[\left(\frac{i(-A_{nk}n + A^*_{nk}n)}{2}\right) - \left(\frac{A^*_{nk}A_{nk}-n^2}{2}\right)\left(\frac{k_q^n n!}{\varepsilon^n}\right)\right]\left[e^{\frac{-2iV_F^n\varepsilon^n}{\gamma^{n-1}}t} - 1\right]\right\} \quad (24)$$

After figuring out the solutions to the aforementioned equations, we can write down the overall average value of the x-axis and y-direction components of the position operator for the AGNRs in the following ways:

$x(t) = \sum_{S,S'=\pm1} x_{S,S'}(t)$ and $y(t) = \sum_{S,S'=\pm1} y_{S,S'}(t)$ (25)

III. DISCUSSION OF RESULTS

This study offers a theoretical analysis of the Zitterbewegung, sometimes called trembling motion, in armchair graphene nanoribbons with one or more layers. First of several parameters that we set up were the pseudo-polarization coefficients (α and β), where α assumed values of 1 and 0 and β was always 1. Graphene sublattice A or B is more likely to contain the electron at the start of motion, depending on these parameters. Secondly, the x and y directions are taken into account by the initial wave vector k, but the y direction's value, $k_{y_0} = 0$, is ignored. k_{x_0} takes on different values as a result of quantised motion in the x-direction, but it is calculated using the long-wave model, which connects it with the nanoribbon width (eq 3). Third, we tested three different values for D, the nanoribbon's width, at $0.52\,nm, 1.04\,nm, and\ 1.55\,nm$. A positive integer M, representing the number of lines that correspond to the positions of atoms in the graphene lattice, is necessary for both the initial wave number k and the width of the nanoribbon D. The original unit cell's hexagon after we computed the predictions for $x(t)$ and $y(t)$ as functions of time. We then used the numerical solutions to equations 17–24 to calculate the expected values of the directions with respect to time, and we displayed this information visually. We calculated the beginning of the trembling motion to be 30 femtoseconds since this phenomenon has a very short lifetime, beginning with the electron's transition between the unit cell's sublattices and the first Brillouin zone, and ending with its decay. As a result, we thought this time value worked well to show the oscillatory motion's increase and decrease in armchair-type graphene nanoribbons. Ribbon length is $L = 200\,nm$, interlayer spacing is $a = 0.124\,nm$ in the hexagonal graphene lattice, and the height between layers is $h = 0.335\,nm$. For different values of the Gaussian bandwidth d and starting wave vectors $k_{y_0} = 0$ and $k_{x_0} = 1.29, 5.77\,nm$, Fig 3 displays the Average expected values of the x and y locations with respect to time for a single graphene nanoribbon layer. The figure further demonstrates that the Average expected values oscillate in both directions depending on the nanoribbon width $D = 0.52\,nm$, as the oscillation amplitude is inversely proportional to the wave packet width. We may also see that the oscillation is periodic and regular at these values. Altering the values of the initial wave vector k_{x_0} did not significantly impact the amplitude or frequency of the oscillation. Zitterbewegung is present in both the transverse and longitudinal directions because the position operators $x(t)$ and $y(t)$ fluctuate.

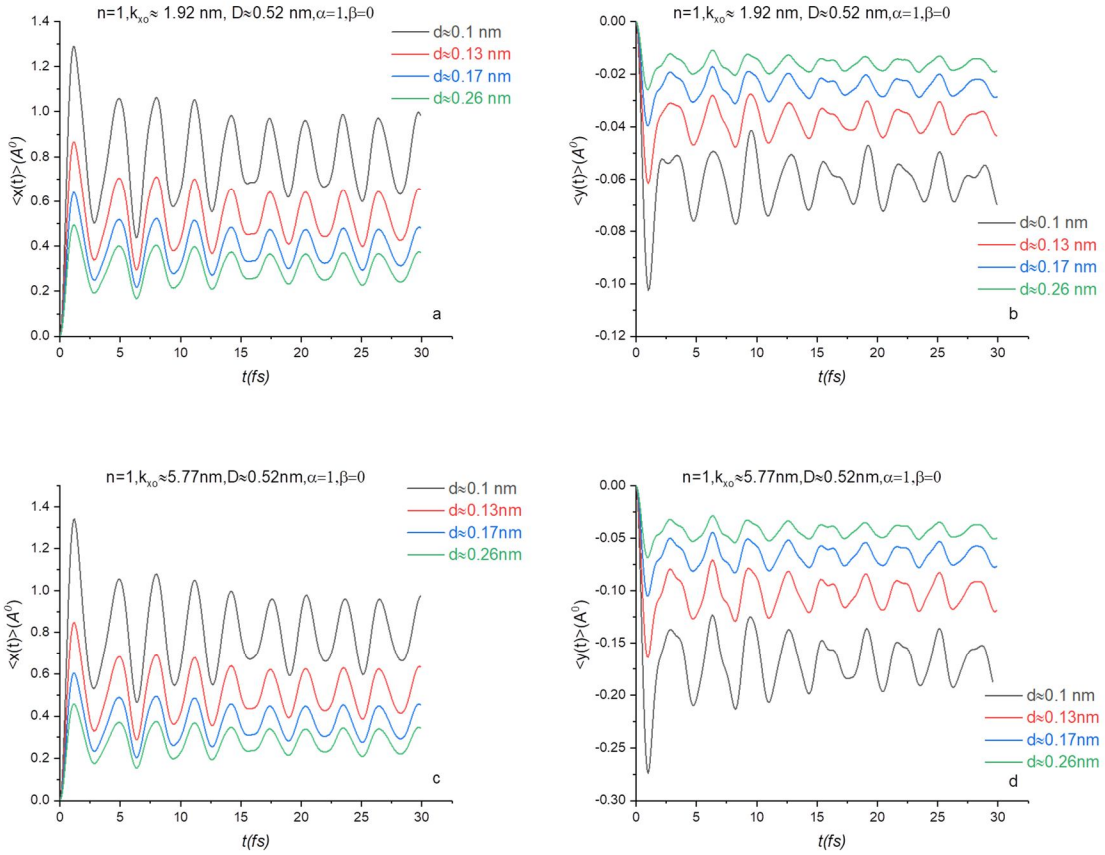

Fig .3. Position operator as a function of time for a single layer of graphene nanoribbon width $D = 0.52\,nm$, $n = 1$, where (a) and (c) represent the longitudinal oscillation with wave vector $k_{x_\circ} \approx 1.92\,nm$, (c) and (d) represent the transverse oscillation with wave vector $k_{x_\circ} \approx 5.77\,nm$, for values of polarisation parameters $\alpha = 1, \beta = 0$, for different values of the Gaussian bandwidth $d = 0.1, 0.13, 0.17, 0.26\,nm$

As a result of setting the pseudo-polarization values to $\alpha = 1$ and $\beta = 1$, it is possible to deduce that the quantum state of the initial motion of electrons in the two sublattices A and B is simultaneous. This implies that the probability of electron presence is the same in both sublattices.

This is seen in fig. 4, where it is clear that there is no fluctuation of the Average expected value in either direction, indicating that the ZBW phenomenon is not realised at these levels.

This is obvious in panels a and b of the figure. While the electrons are in their initial motion, there is no constructive interference between the wave and the negative energy values. As a consequence, there is a linear connection between the position values and the time.

An increase in the starting wave vector $k_{x_\circ}$ causes this linearity to become more evident, as seen in fig.4 (c, d). As was mentioned before, this does not have a direct impact on the oscillation, which decreases as time t continues, suggesting that motion is still occurring.

International Journal for Research in Applied Science & Engineering Technology (IJRASET)
ISSN: 2321-9653; IC Value: 45.98; SJ Impact Factor: 7.538
Volume 13 Issue III Mar 2025- Available at www.ijraset.com

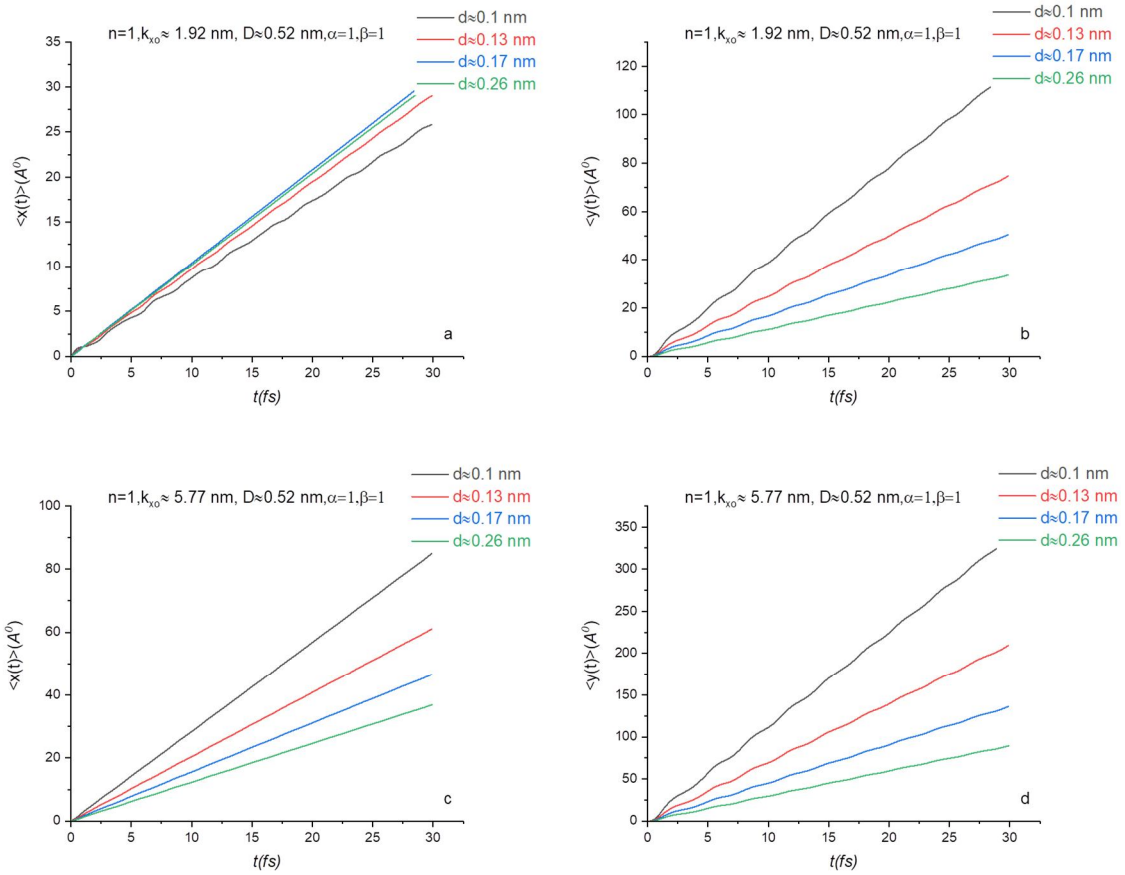

Fig .4. Position operator as a function of time for a single layer of graphene nanoribbon width $D = 0.52\,nm$, $n = 1$, where (a) and (c) represent the longitudinal oscillation with wave vector $k_{x\circ} \approx 1.92\,nm$, (c) and (d) represent the transverse oscillation with wave vector $k_{x\circ} \approx 5.77\,nm$, for values of polarisation parameters $\alpha = 1, \beta = 1$, for different values of the Gaussian bandwidth $d = 0.1, 0.13, 0.17, 0.26\,nm$

When the width of the graphene nanoribbon is increased to $D = 1.04\,nm$, as shown in fig.5, we detect a consistent and steady oscillation behaviour that is comparable to the one shown in fig.3. The starting wave vector $k_{x\circ}$ does not seem to have any noticeable influence; nevertheless, the width of the nanoribbon led to a drop in the maximum oscillation amplitude, which went from $1.4A^{\circ}$ in to $1.2A^{\circ}$ in. Fig.5 displays the data that demonstrates the irregularity of the oscillation period at the beginning of the movement. This is something that we also see.

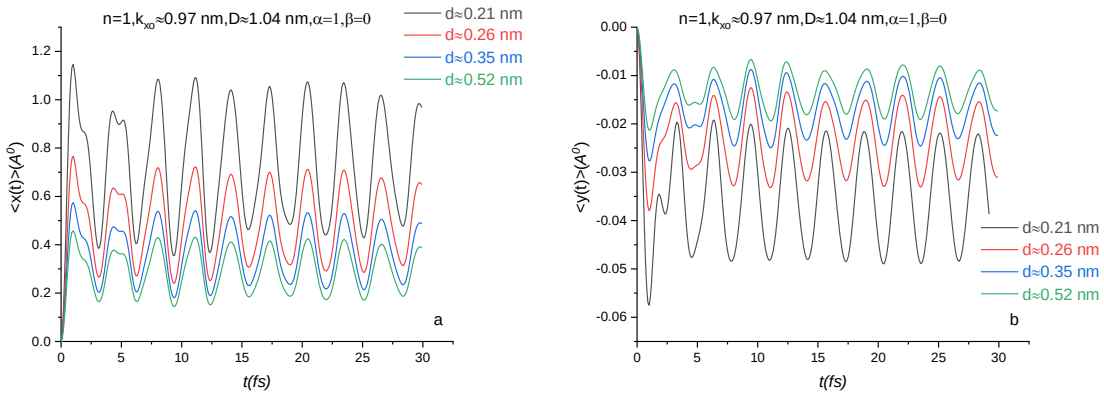

International Journal for Research in Applied Science & Engineering Technology (IJRASET)
ISSN: 2321-9653; IC Value: 45.98; SJ Impact Factor: 7.538
Volume 13 Issue III Mar 2025- Available at www.ijraset.com

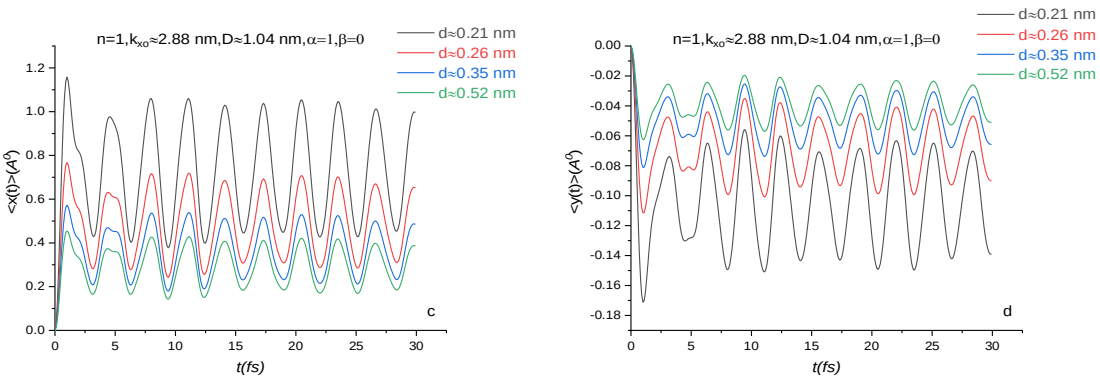

Fig .5. Position operator as a function of time for a single layer of graphene nanoribbon width $D = 1.04\,nm$, $n = 1$,where (a) and (c) represent the longitudinal oscillation with wave vector $k_{x_\circ} \approx 2.88\,nm$, (c) and (d) represent the transverse oscillation with wave vector $k_{x_\circ} \approx 2.88\,nm$, for values of polarisation parameters $\alpha = 1, \beta = 0$, for different values of the Gaussian bandwidth $d = 0.21,0.26,0.35,0.52\,nm$

In the case of an armchair nanoribbon with a width of $D = 0.52\,nm$, where $\alpha = 1$ and $\beta = 0$, the oscillatory behaviour consistently occurs in both the longitudinal and transverse orientations. The figures c and d in fig.4 demonstrate that linear oscillation is readily apparent when the values of α and β are equal to one. This phenomenon takes place in a transverse orientation that is directly proportional to the width of the wave packet, while in the longitudinal direction, it is inversely proportional. In fig 6, we can see that an armchair graphene nanoribbon with $D = 1.55\,nm$ has oscillatory behaviour. Figus.5(a, b) demonstrate that when the parameters $\alpha = 1$ and $\beta = 0$, the longitudinal oscillation seems to be relatively unequal. On the other hand, the transversal oscillation is transitory and has a modest amplitude. Fig.6(c, d) demonstrate that the conductive armchair graphene nanoribbon with $D = 0.52\,nm$ showed linear oscillation at $\alpha = \beta = 1$. This is apparent in the graph.

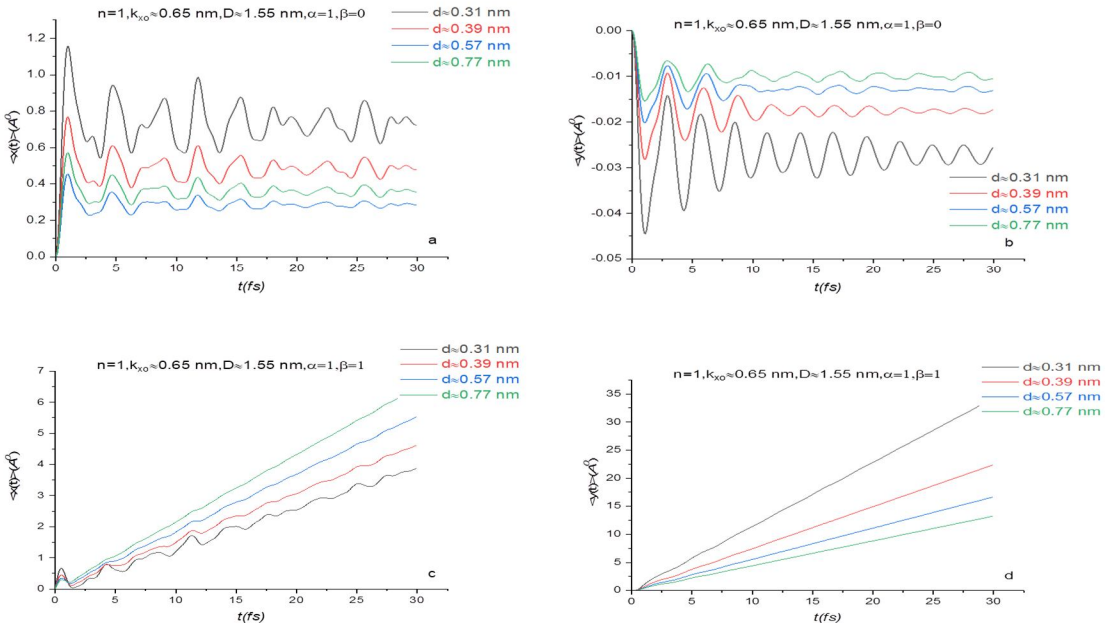

Fig .6. Position operator as a function of time for a single layer of graphene nanoribbon width $D = 1.55\,nm$, $n = 1$, where (a) and (c) represent the longitudinal oscillation with wave vector $k_{x_\circ} \approx 0.65\,nm$, for values of polarisation parameters $\alpha = 1, \beta = 0$ (c) and (d) represent the transverse oscillation with wave vector $k_{x_\circ} \approx 0.65\,nm$, for values of polarisation parameters $\alpha = 1, \beta = 1$, for different values of the Gaussian bandwidth $d = 0.31,0.39,0.57,0.77\,nm$

©IJRASET: All Rights are Reserved

Figs.7(a, b) illustrate the oscillatory behaviour of the longitudinal and transverse average expected value, also known as zitterbewegung, for a bilayer of armchair graphene nanoribbon. These figures were created using two distinct values of the pseudopolarization parameters, $\alpha = 1, \beta = 0$. In the middle of the time period, the oscillation lasts for around 15 femtoseconds, after which it practically vanishes and then returns with a significant amplitude. The hopping energy parameter, which has a value of $0.377\ meV$, is likely to have a part in this phenomenon. This is due to the fact that electrons lose energy as they go from one layer to the next. It is clear that the amplitude has grown by a factor of three when we compare these two figures with Fig.3(a, b). Additionally, the frequency value has also increased, which demonstrates how the layer multiplicity influences the zitterbewegung frequency. However, in the case of the bilayer, a frequency with a significant amplitude occurs at the beginning of movement. This is seen in Figs.7(c, d), which indicate that linear behaviour resumes when $\alpha = 1, \beta = 1$. At a time, interval of around 5 femtoseconds, the longitudinal and transverse movements both display consistent linear behaviour. In spite of the fact that the initial wave vector $k_{x_\circ}$ did not seem to have much of an impact, the component that stands out the most is the wave packet width d. This is because the amplitude has a tendency to grow as the width decreases.

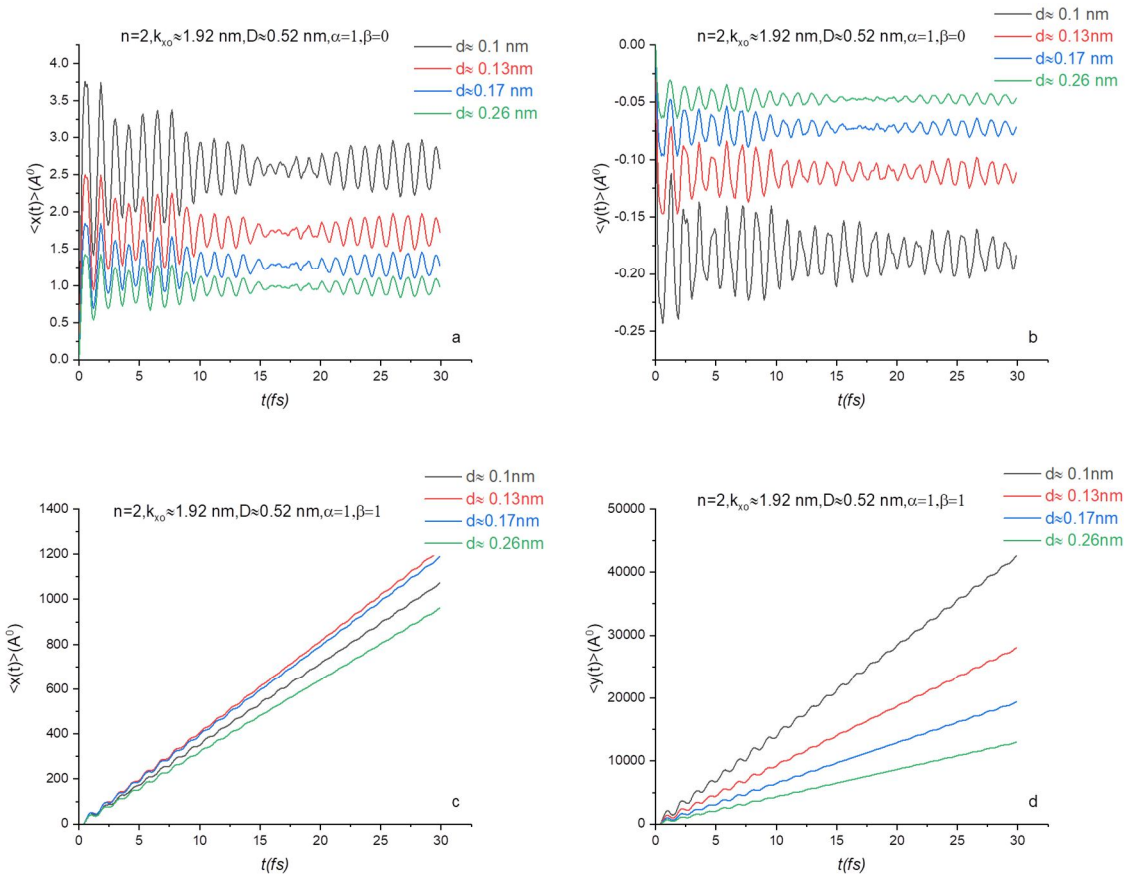

Fig .7. Position operator as a function of time for a monolayer of graphene nanoribbon width $D = 0.52\ nm$, $n = 2$,where (a) and (c) represent the longitudinal oscillation with wave vector $k_{x_\circ} \approx 1.92\ nm$, for values of polarisation parameters $\alpha = 1, \beta = 0$ (c) and (d) represent the transverse oscillation with wave vector $k_{x_\circ} \approx 1.92\ nm$, for values of polarisation parameters $\alpha = 1, \beta = 1$, for different values of the Gaussian bandwidth $d = 0.1, 0.13, 0.17, 0.26\ nm$.

The influence of increasing the width of the armchair graphene nanoribbon on the time evolution of the wave packet at $D = 1.04\ nm$ was investigated in fig.8 (a, b, c, d). This was done while maintaining consistent values for the other parameters, as shown in fig.7. This was accomplished by graphing the average expected value against time for both longitudinal and transverse oscillations. At $D = 0.52\ nm$, the oscillation displays a typical behaviour that is comparable to that of the other oscillations.

However, a significant distinction emerges in the fact that, as the width of the nanoribbon increases, the oscillation decreases at a faster rate, especially in the transverse direction, as shown in fig.8(a). In comparison to fig.7(b), the oscillation in the longitudinal direction has a period that is more regular, and the rate at which it decays is slower than the rate at which it decays in the transverse direction. When comparing fig.8 with fig.5, it is possible to see an increase in the oscillation amplitude value. This occurs when the nanoribbon changes to a bilayer structure. We find the appearance of linear oscillatory activity with regard to $\alpha = 1, \beta = 1$, for example, as shown in fig.8(c, d). However, the frequency of this behaviour is lower than that of fig.7(c, d). The oscillation of the predicted value of the site in the transverse direction needs a length that is longer than thirty femtoseconds in order for the electron hopping region to become visible between the layers before the oscillatory movement may resume. With regard to this particular system, the double layer is superior to the single layer since it is capable of producing higher capacity and improved oscillation, both of which are desirable characteristics.

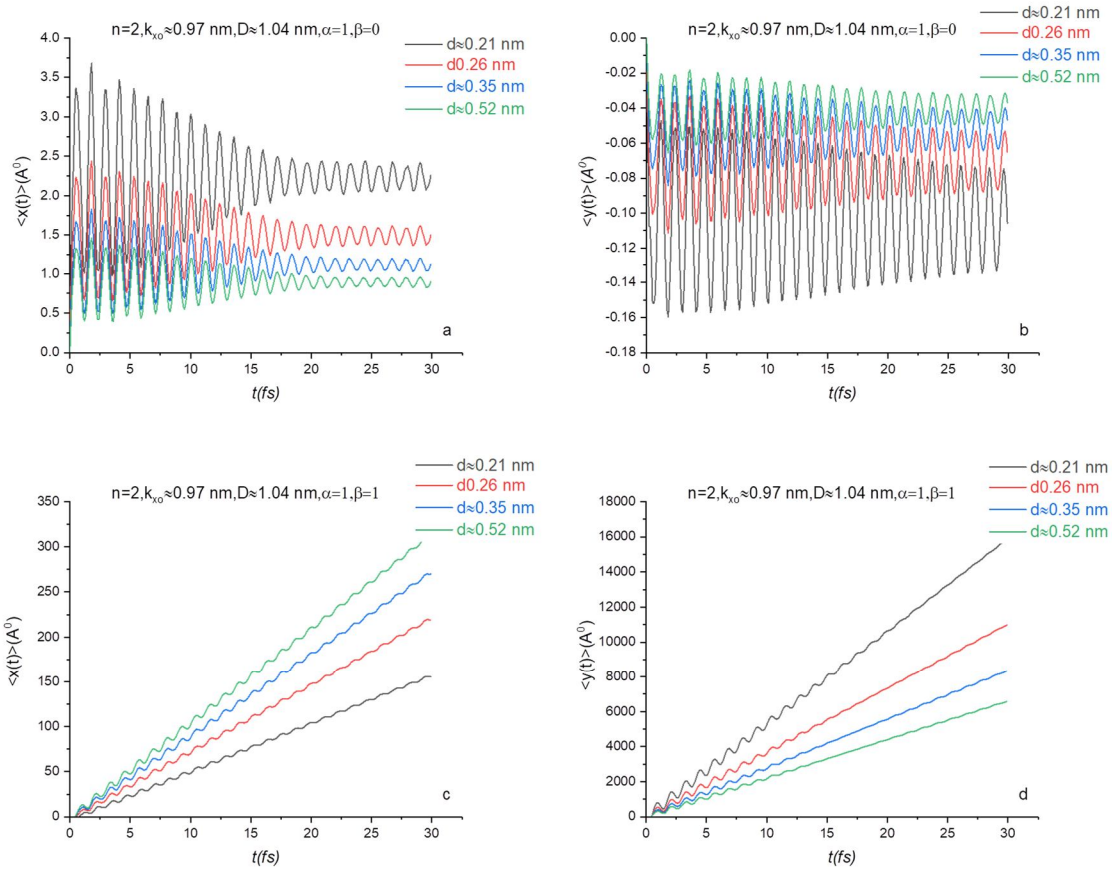

Fig .8. Position operator as a function of time for a monolayer of graphene nanoribbon width $D = 0.97\,nm$, $n = 2$,where (a) and (c) represent the longitudinal oscillation with wave vector $k_{x_\circ} \approx 0.97\,nm$, for values of polarisation parameters $\alpha = 1, \beta = 0$ (c) and (d) represent the transverse oscillation with wave vector $k_{x_\circ} \approx 0.97\,nm$, for values of polarisation parameters $\alpha = 1, \beta = 1$, for different values of the Gaussian bandwidth $d = 0.21, 0.26, 0.35, 0.52\,nm$.

Fig.9 depicts the oscillatory behaviour of the bilayer; it is pretty similar to fig .8, with the exception that the width is $D = 1.55\,nm$ and the parameters are the same as in fig 8. As seen in figs.9(a, b), the breadth of the wave packet decreases after a brief time of oscillation. This is the case for the parameters $\alpha = 1, \beta = 0$. In light of this, the moment at which the linear oscillation occurred was at the point when $\alpha = 1, \beta = 1$. The observation that the rate of oscillation decay accelerates at a quicker rate than previously recorded, as shown in fig.9(b), is what differentiates fig.9 from fig.8. This is because the width of the graphene nanoribbon increases. The trembling motion does not exhibit periodic regularity, and the oscillation is also non-linear in the transverse direction, which is a strong indication that randomness is beginning to emerge. Both Fig.6(a, b) provide the identical finding for our perusal.

©IJRASET: All Rights are Reserved

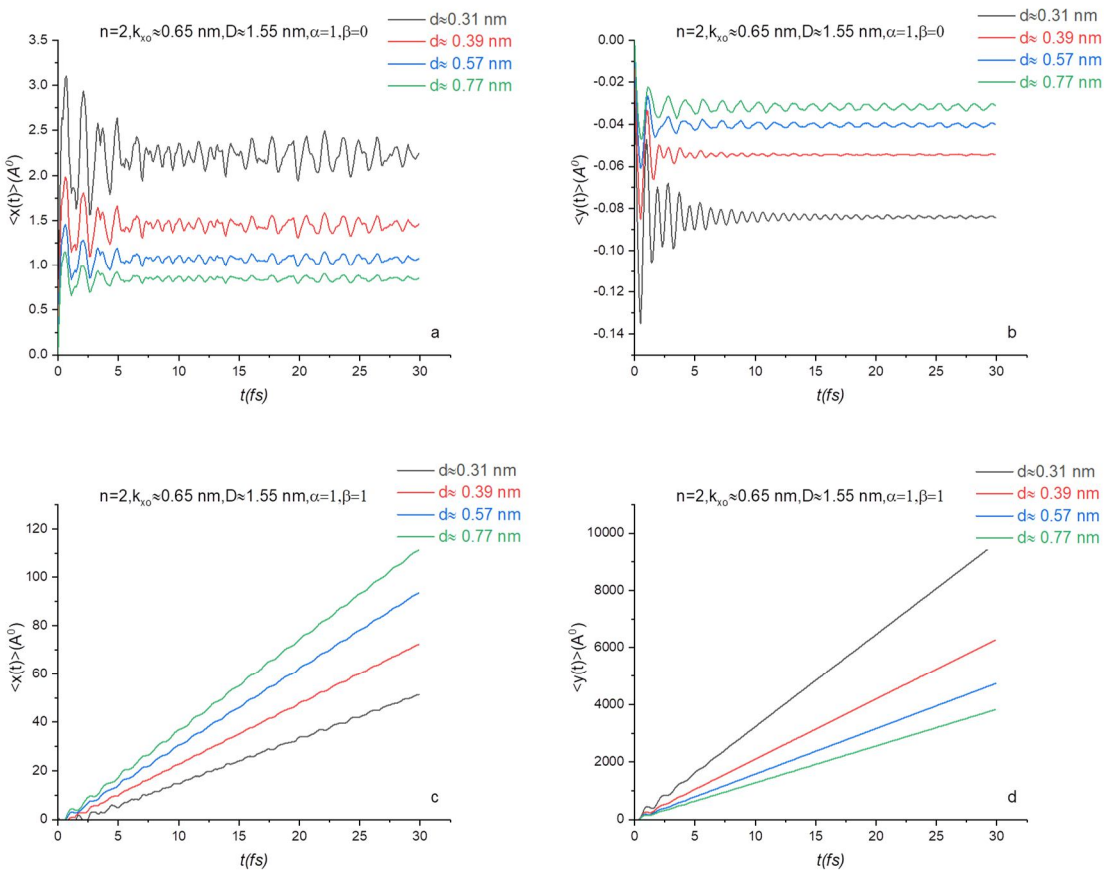

Fig .9. Position operator as a function of time for a monolayer of graphene nanoribbon width $D = 1.55\,nm$, $n = 2$,where (a) and (c) represent the longitudinal oscillation with wave vector $k_{x\circ} \approx 0.65\,nm$, for values of polarisation parameters $\alpha = 1, \beta = 0$ (c) and (d) represent the transverse oscillation with wave vector $k_{x\circ} \approx 0.65\,nm$, for values of polarisation parameters $\alpha = 1, \beta = 1$, for different values of the Gaussian bandwidth $d = 0.31, 0.39, 0.57, 0.77\,nm$.

The oscillatory behaviour of a trilayer armchair graphene nanoribbon was examined in Figs. 10, 11, and 12 for varying widths of $D = 0.52, 1.04, and\ 1.55\,nm$. The figures illustrate that the oscillation behaviour resembles that of the bilayer; nevertheless, it is characterised by bigger transient oscillations that cease during layer transitions, resulting in two areas where oscillation is lost. The impact of multilayering is evident, since the oscillation decay occurs more rapidly than previously seen. The optimal results were achieved with $n = 2$ layers and a nanoribbon width of $D = 1.04, 0.52\,nm$, with $\alpha = 1, \beta = 0$ for longitudinal and transverse oscillations, characterised by a high frequency and regular periodicity.

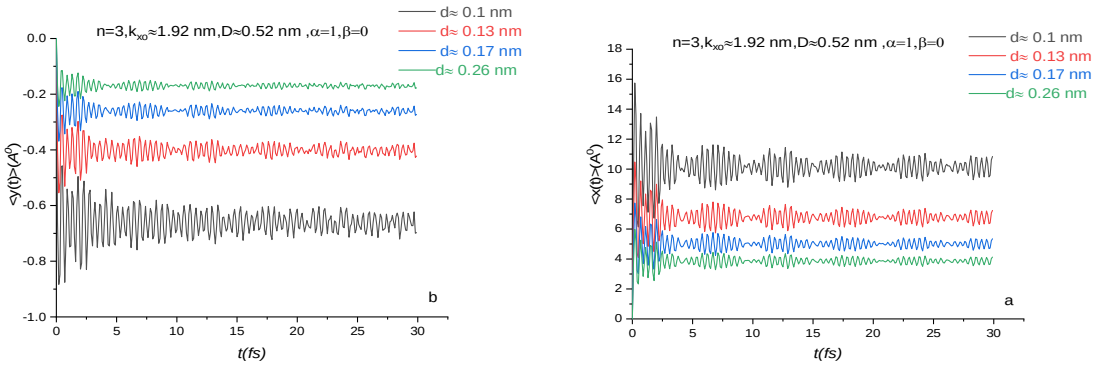

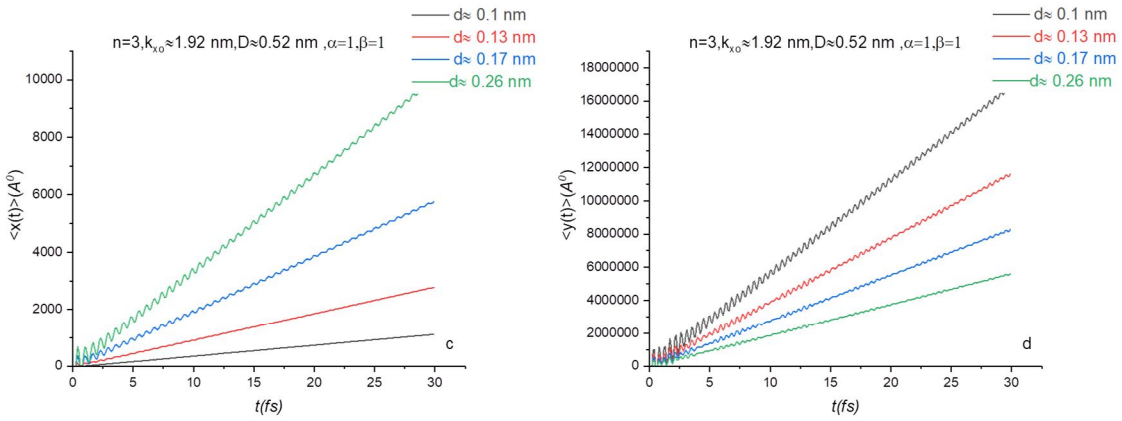

Fig .10. Position operator as a function of time for a trilateral of graphene nanoribbon width $D = 0.52\,nm$, $n = 3$, where (a) and (c) represent the longitudinal oscillation with wave vector $k_{x_\circ} \approx 1.92\,nm$, for values of polarisation parameters $\alpha = 1, \beta = 0$ (c) and (d) represent the transverse oscillation with wave vector $k_{x_\circ} \approx 1.92\,nm$, for values of polarisation parameters $\alpha = 1, \beta = 1$, for different values of the Gaussian bandwidth $d = 0.1,0.13,0.17,0.26\,nm$.

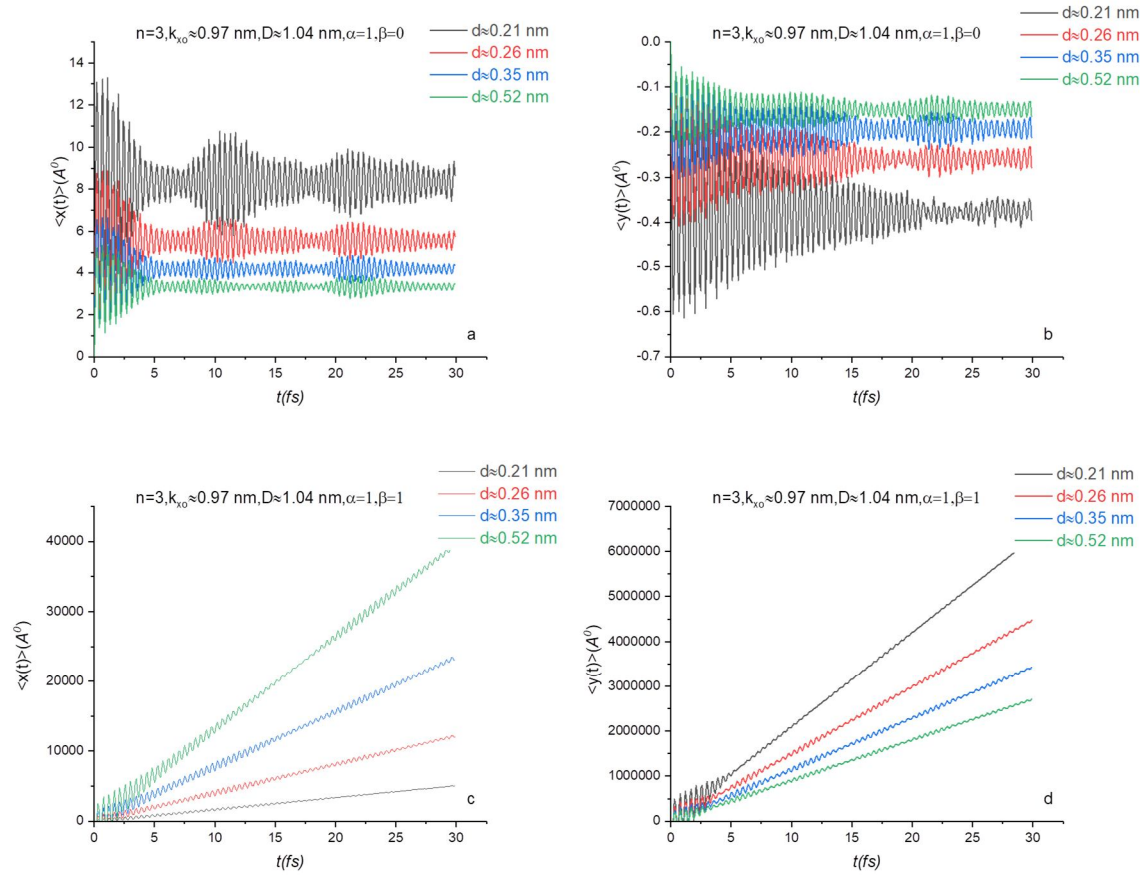

Fig .11. Position operator as a function of time for a trilateral of graphene nanoribbon width $D = 1.04\,nm$, $n = 3$,where (a) and (c) represent the longitudinal oscillation with wave vector $k_{x_\circ} \approx 0.97\,nm$, for values of polarisation parameters $\alpha = 1, \beta = 0$ (c) and (d) represent the transverse oscillation with wave vector $k_{x_\circ} \approx 0.97\,nm$, for values of polarisation parameters $\alpha = 1, \beta = 1$, for different values of the Gaussian bandwidth $d = 0.21,0.26,0.35,0.52\,nm$.

©IJRASET: All Rights are Reserved

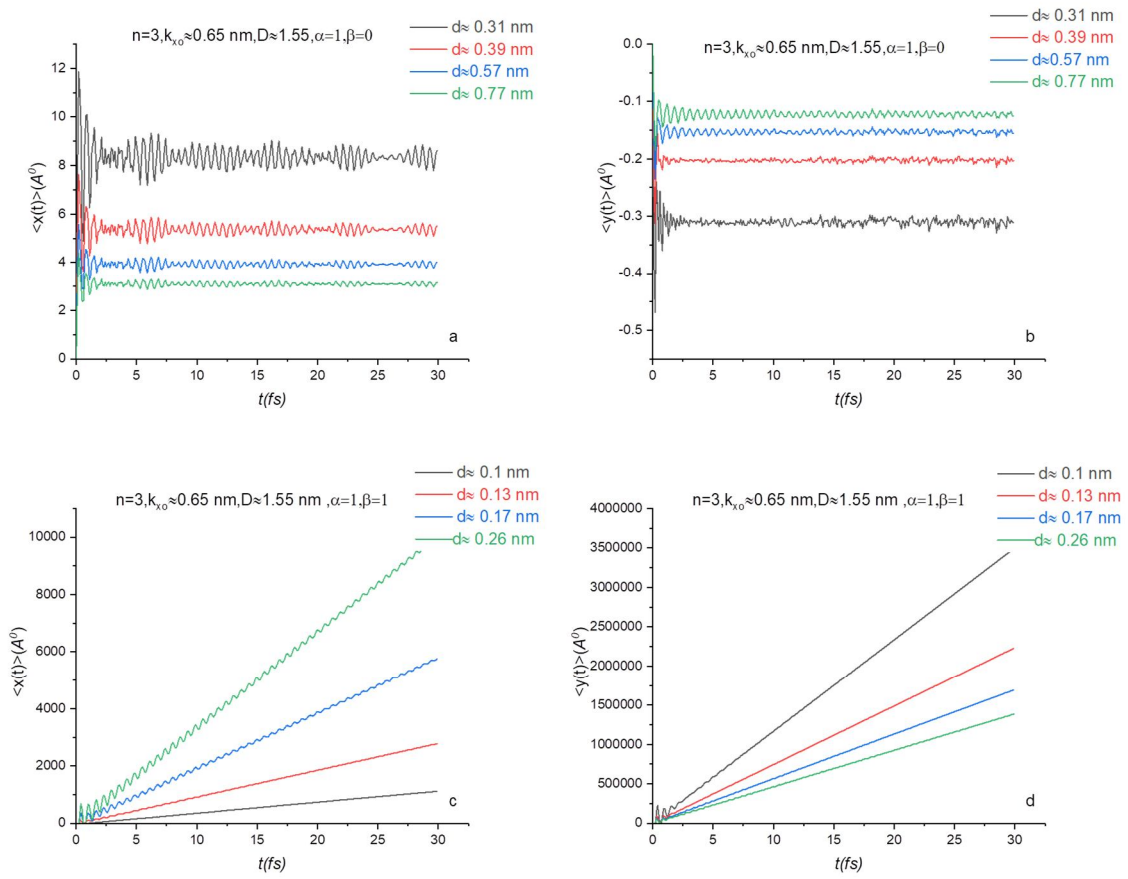

Fig .12. Position operator as a function of time for a trilateral of graphene nanoribbon width $D = 1.55\,nm$, $n = 3$,where (a) and (c) represent the longitudinal oscillation with wave vector $k_{x\circ} \approx 0.65\,nm$, for values of polarisation parameters $\alpha = 1, \beta = 0$ (c) and (d) represent the transverse oscillation with wave vector $k_{x\circ} \approx 0.65\,nm$, for values of polarisation parameters $\alpha = 1, \beta = 1$, for different values of the Gaussian bandwidth $d = 0.31, 0.39, 0.57, 0.77\,nm$.

IV. FINAL CONCLUSIONS

The phenomena of trembling motion, referred to as zitterbewegung, in both single and multilayer graphene, along with other intriguing features of graphene, is a compelling subject that has garnered much theoretical investigation. This research paper contributes to theoretical studies aimed at verifying the feasibility of realising the zitterbewegung (ZBW) phenomenon in armchair graphene nanoribbons, utilising a theoretical framework grounded in the Heisenberg representation of position operators for the Gaussian wave packet of relativistic Dirac electrons. We also used the Schrödinger methodology to compute the anticipated values and elucidate the manifestation of this phenomena in graphene nanoribbons. We investigated the influence of various parameters on the oscillatory motion of electrons, specifically the width of the nanoribbon D, the initial longitudinal wave vector $k_{x\circ}$, the pseudo-spin polarizabilities (alpha and beta) indicating the likelihood of an electron residing in either sublattice A or B of the graphene honeycomb, the number of layers n, and the width of the Gaussian beam d. The pseudo-spin polarisability parameters exhibit two distinct kinds of oscillations based on their values: transverse oscillation and quasi-linear oscillation. Consequently, these parameters may be regarded as very influential in this occurrence. The Gaussian bandwidth values had no significant impact, save for an inverse association between the bandwidth and the oscillation amplitude. The influence of the start wave vector $k_{x\circ}$ did not manifest in the amplitude or oscillation values distinctly; nonetheless, it affected the regular periodicity of the oscillation, with larger values yielding a more consistent first oscillation.

The width of the graphene nanoribbon *D* significantly influenced the oscillation frequency values; specifically, an increase in width correlated with a higher frequency and a reduced amplitude when transitioning from single-layer to multi-layer graphene. Incorporating the number of layers into the calculations revealed a quasi-regular periodic increase in oscillation frequency, particularly evident in the bilayer, while this regularity diminished in the trilayer. Overall, for all the parameters discussed, the observed oscillation was intrinsic, devoid of external influence, characterised by its transient nature within a duration of 30 femtoseconds. This phenomenon may be regulated by the values of the initial wave vector $k_{x_\circ}$ by the selection of suitable values and the width of the graphene nanoribbon. The findings of this study work may enhance the comprehension of the zitterbewegung phenomena in these systems. The manifestation of this phenomena in graphene nanoribbons may significantly enhance the comprehension of some intriguing features of graphene, particularly as it occurs in armchair-edged nanoribbons. We anticipate its use in the production of large-capacity computer processors owing to the very high frequency of this phenomena. This discovery may also be beneficial for future investigations into zigzag graphene ribbons to validate the zitterbewegung phenomena and other features.

REFERENCES

[1] Rusin, Tomasz M., and Wlodek Zawadzki. "Two-photon echo method for observing electron zitterbewegung in carbon nanotubes." Semiconductor Science and Technology 29.12 (2014): 125010.
[2] Chen, Ying. PATTERNING ELASTOMER, THERMOPLASTICS AND SHAPE MEMORY MATERIAL BY UVO LITHOGRAPHY AND SOFT LITHOGRAPHY. Diss. University of Akron, 2017.
[3] Ghosh, S., Udo Schwingenschlögl, and Aurelien Manchon. "Resonant longitudinal Zitterbewegung in zigzag graphene nanoribbons." Physical Review B 91.4 (2015): 045409.
[4] Cunha, S. M., et al. "Wave-packet dynamics in multilayer phosphorene." Physical Review B 99.23 (2019): 235424.
[5] Montambaux, Gilles. "Artificial graphenes: Dirac matter beyond condensed matter." Comptes Rendus Physique 19.5(2018): 285-305.
[6] Wang, Yi-Xiang, Yue-Juan He, and Shi-Jie Xiong. "Study of Zitterbewegung and the Radiated Fields in Graphene System." Modern Physics Letters B 26.21 (2012): 1250139.
[7] Lavor, I. R., et al. "Effect of zitterbewegung on the propagation of wave packets in ABC-stacked multilayer graphene: an analytical and computational approach." Journal of Physics: Condensed Matter 33.9 (2020): 095503.
[8] Biswas, Tutul, and Tarun Kanti Ghosh. "Zitterbewegung of electrons in quantum wells and dots in the presence of an in-plane magnetic field." Journal of Physics: Condensed Matter 24.18 (2012): 185304.
[9] Schliemann, John, Daniel Loss, and R. M. Westervelt. "Zitterbewegung of electronic wave packets in III-V zinc- blende semiconductor quantum wells." Physical review letters 94.20 (2005): 206801.
[10] Schliemann, John, Daniel Loss, and R. M. Westervelt. "Zitterbewegung of electrons and holes in III–V semiconductor quantum wells." Physical Review B—Condensed Matter and Materials Physics 73.8 (2006): 085323.
[11] Zawadzki, Wlodek, and Tomasz M. Rusin. "Zitterbewegung (trembling motion) of electrons in semiconductors: a review." Journal of Physics: Condensed Matter 23.14 (2011): 143201.
[12] Biswas, Tutul, Sandip Chowdhury, and Tarun Kanti Ghosh. "Zitterbewegung of a heavy hole in presence of spin- orbit interactions." The European Physical Journal B 88 (2015): 1-6.
[13] Novoselov, Kostya S., et al. "Electric field effect in atomically thin carbon films." science 306.5696 (2004): 666-669.
[14] Novoselov, Kostya S., et al. "Two-dimensional gas of massless Dirac fermions in graphene." nature 438.7065 (2005): 197-200.
[15] M. I. Katsnelson, The European physical Journal B, 51, 157 (2006).
[16] Rusin, Tomasz M., and Wlodek Zawadzki. "Transient Zitterbewegung of charge carriers in mono-and bilaye graphene, and carbon nanotubes." Physical Review B—Condensed Matter and Materials Physics 76.19 (2007): 195439.
[17] Majid, M. J., and S. S. Savinskii. "Features of the time evolution of localized quantum states in graphene." Semiconductors 47 (2013): 141-145.
[18] Mahan, Munera W., and M. J. Majid. "Time Evolution of the Position Operators in a Bilayer Graphene." NeuroQuantology 19.12 (2021): 19.
[19] Majid, M. J., and M. H. Alaa. "Time evolution of current density in conducting single-walled carbon nanotubes." Journal of Computational Electronics 17 (2018): 595-603.
[20] Majid, M. J., and M. H. Alaa. "JOURNAL OF KUFA− PHYSICS."
[21] Majid, M. J., and M. H. Alaa. "Trembling motion of the wave packet in armchair graphene nanoribbons (AGNRs)." International Journal of Modern Physics B 32.32 (2018): 1850364.
[22] Mahan, Munera W., and M. J. Majid. "Time Evolution of the Position Operators in a Bilayer Graphene." NeuroQuantology 19.12 (2021): 19.
[23] Lavor, I. R., et al. "Effect of zitterbewegung on the propagation of wave packets in ABC-stacked multilayer graphene: an analytical and computational approach." Journal of Physics: Condensed Matter 33.9 (2020): 095503.

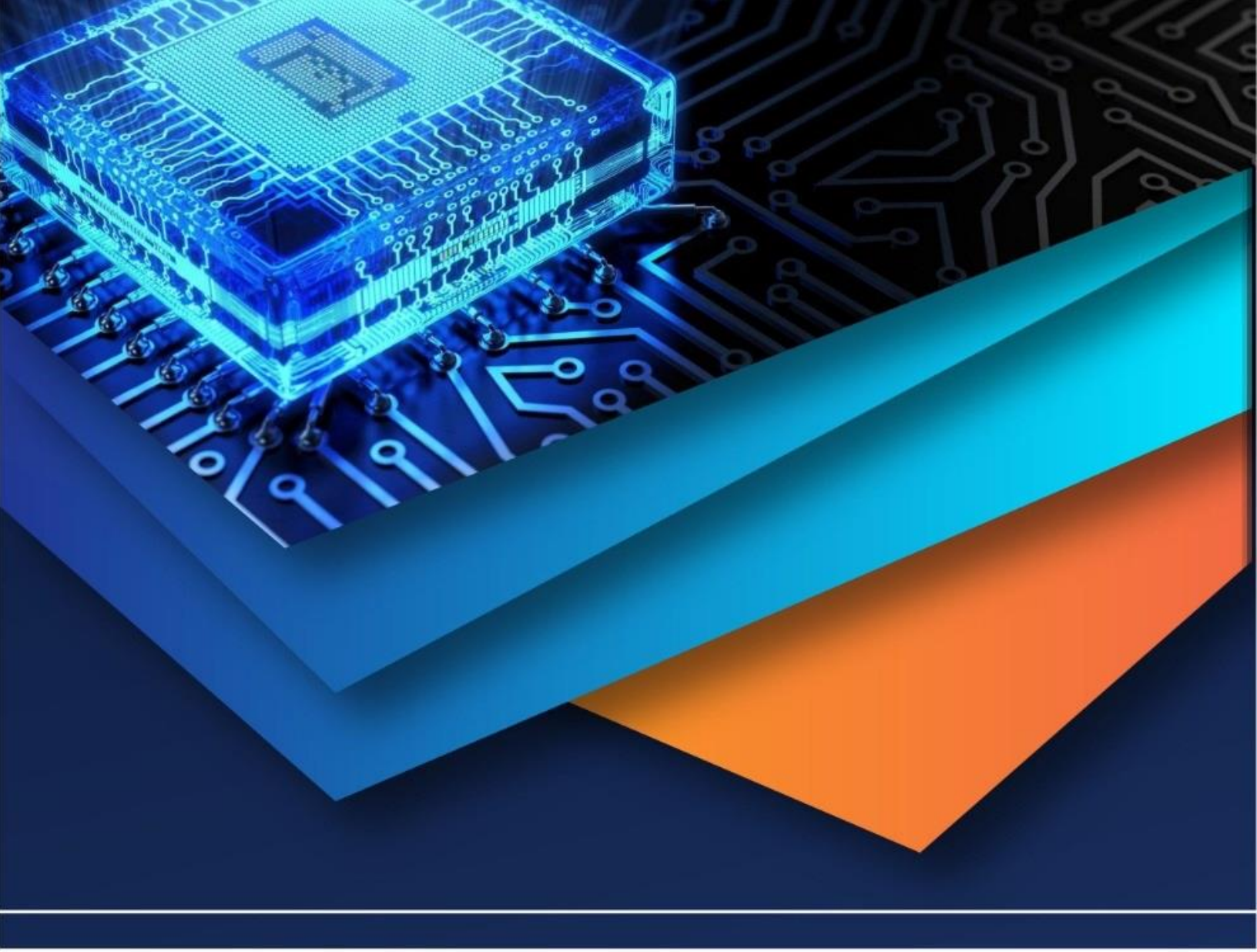

10.22214/IJRASET

45.98

IMPACT FACTOR: 7.129

IMPACT FACTOR: 7.429

INTERNATIONAL JOURNAL FOR RESEARCH

IN APPLIED SCIENCE & ENGINEERING TECHNOLOGY

Call : 08813907089 (24*7 Support on Whatsapp)